Supplementary Table 1

Header: Quality control and exclusion of BH runs

Caption: Individual reasons of exclusion of a BH run are listed.

Supplementary Table 2

Header: Statistical tests for differences in MREG, HR, NIBP, and NIRS signal amplitudes before versus after BH

Caption: For signals in Figure 2, Figure 3 and Supplementary figure 2 averages of 10 seconds before BH and 10 seconds after BH for each good BH were compared using a Wilcoxon signed rank test with Bonferroni correction for the respective number of multiple comparisons (significance level after Bonferroni correction: Figure 3 and Supplementary Figure 2: alpha = 0.0056).

Supplementary Table 3

Header: Statistical tests on spatial similarity of QPP maps

Caption: The upper part lists results of non-parametric two-sided paired-samples Wilcoxon signed rank tests (significance level after Bonferroni correction: alpha = 0.005) comparing spatial correlation coefficients between QPP maps of BH with the respective NV0 for every subject (Figure 5B). The lower part lists results of non-parametric two-sided two-samples Wilcoxon rank sum tests (significance level after Bonferroni correction: alpha = 0.01) comparing spatial correlation coefficients between QPP maps of BH with the respective NV0 for every subject (Supplementary Figure 2).

Supplementary Figure 1

Experimental paradigm: Normoventilation (NV0, 40 s) is followed by 5 runs of breath holding (BH1-5, 32s) and recuperative NV (NV1-5, 88s).

Supplementary Figure 2

Cardiovascular pulse amplitude of MREG signal during BH from ICA-based ROIs (primary visual network (Visual), DMNpcc, DMNvmpf, white matter (WM) and cerebrospinal fluid (CSF)). The grey box marks the 32 s BH period. Black lines represent mean signal amplitude and the shaded dark grey error bars represent standard deviation. Selected ROIs did not show changes in signal amplitude following BH compared to preceding NV after Bonferroni correction. Significance level after Bonferroni correction $p<0.0056$ (***).

Supplementary Figure 3

QPP maps during BH were compared to an independent resting-state MREG dataset, where 13 subjects (7 females, mean age: 40.15 years) performed continuous ad lib respiration. The imaging parameters, preprocessing, and QPP analysis steps were identical, except for a slightly shorter scan duration of around 600 s. The timecourses were split into six consecutive 20 s (200 timepoints) segments. Correlation coefficients between respective BH and Resting State segments were checked for differences using non-parametric two-samples Wilcoxon rank sum test (MATLAB *ranksum,* significance level after Bonferroni correction: alpha = 0.01, Supplementary Table 3). 4D spatial correlation of cardiovascular QPP map between BH1–5 and NV0 (colored boxes) and five successive resting-state time intervals derived from an independent sample of subjects performing ad lib respiration (grey boxes). On each box, the line and square indicate the median and mean, respectively and the bottom and top edges of the box indicate the 25^{th} and 75^{th} percentiles, respectively. Whiskers extend to the

5th and 95th percentiles and minimum and maximum values most extreme data points and outliers are plotted as 'x'. Bars indicate a significant difference between respective BHs and resting states, with *: p<0.01 and **: p<0.001, Bonferroni corrected.

Supplementary Figure 4

Average QPP amplitude maps of cardiovascular pulse of each of the five breath-holds (BH1-5). For each subject QPP maps over 20 second period during BH were calculated and z-score normalized. Z-score thresholds of 1 and 3 were chosen to make it easier to interpret changes of pulse propagation between different BH runs.

Supplementary Figure 5

Average QPP amplitude maps of cardiovascular pulse of each of the six normo-ventilation segments (NV0-5). For each subject QPP maps were calculated from 20 second period from the beginning before any BH runs (NV0) and 20 second periods 48 second after BH run (NV1-5). Z-score thresholds of 1 and 3 were chosen to make it easier to interpret changes of pulse propagation between different BH runs.

Supplementary Figure 6

Replication of the main effect of cardiac pulse amplitudes with additionally applied AFNI *3dDespike NEW25*, an aggressive spike removal method to investigate possible contribution of subject motion as a confounding factor. Clusters in the pre-Bötzinger complex, pneumotaxic and apneustic centers remained, the thalamus cluster even enlarged, but clusters previously observed in hypothalamus as well as dorsal and ventral respiratory group vanished.

Supplementary_figure_1

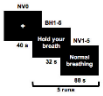

Supplementary_figure_2

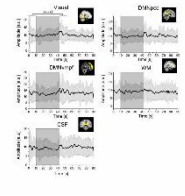

Supplementary_figure_3

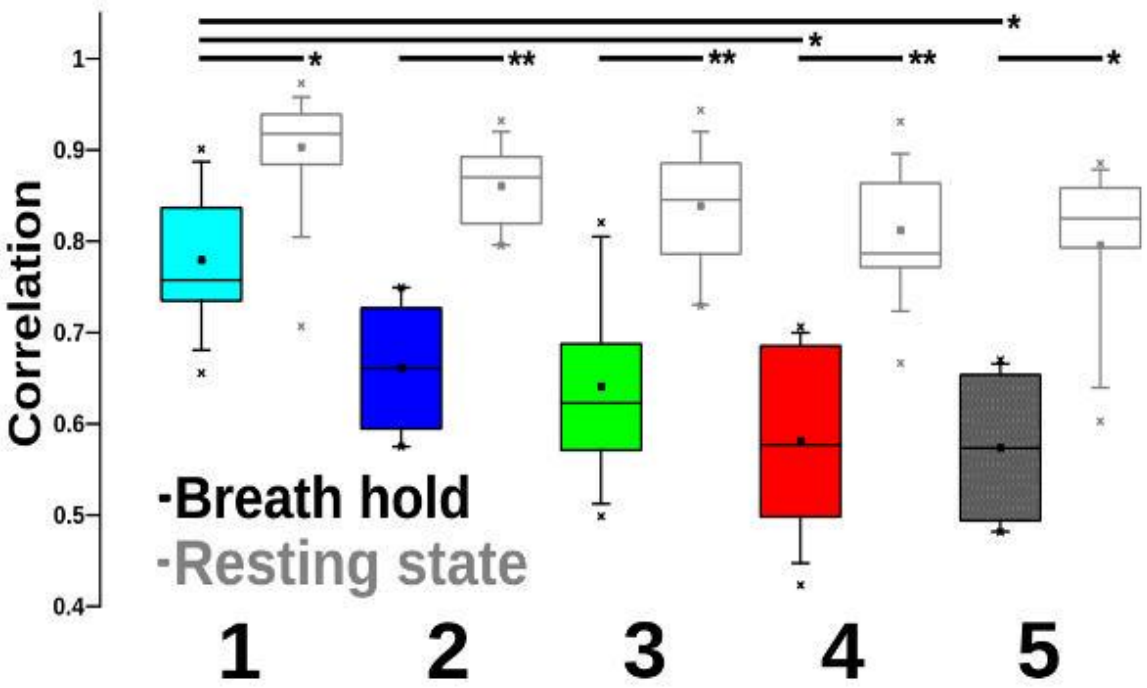

Supplementary_figure_4

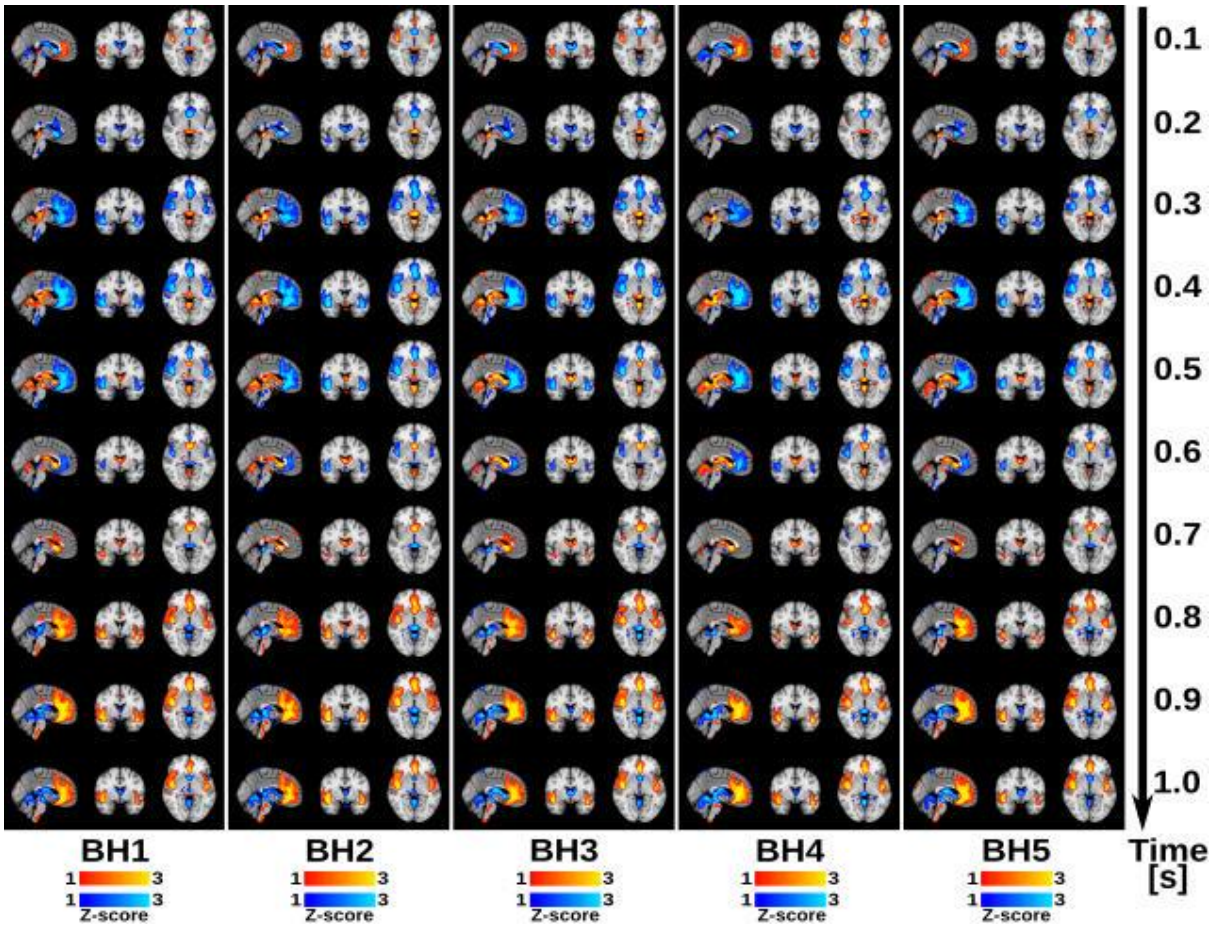

Supplementary_figure_5

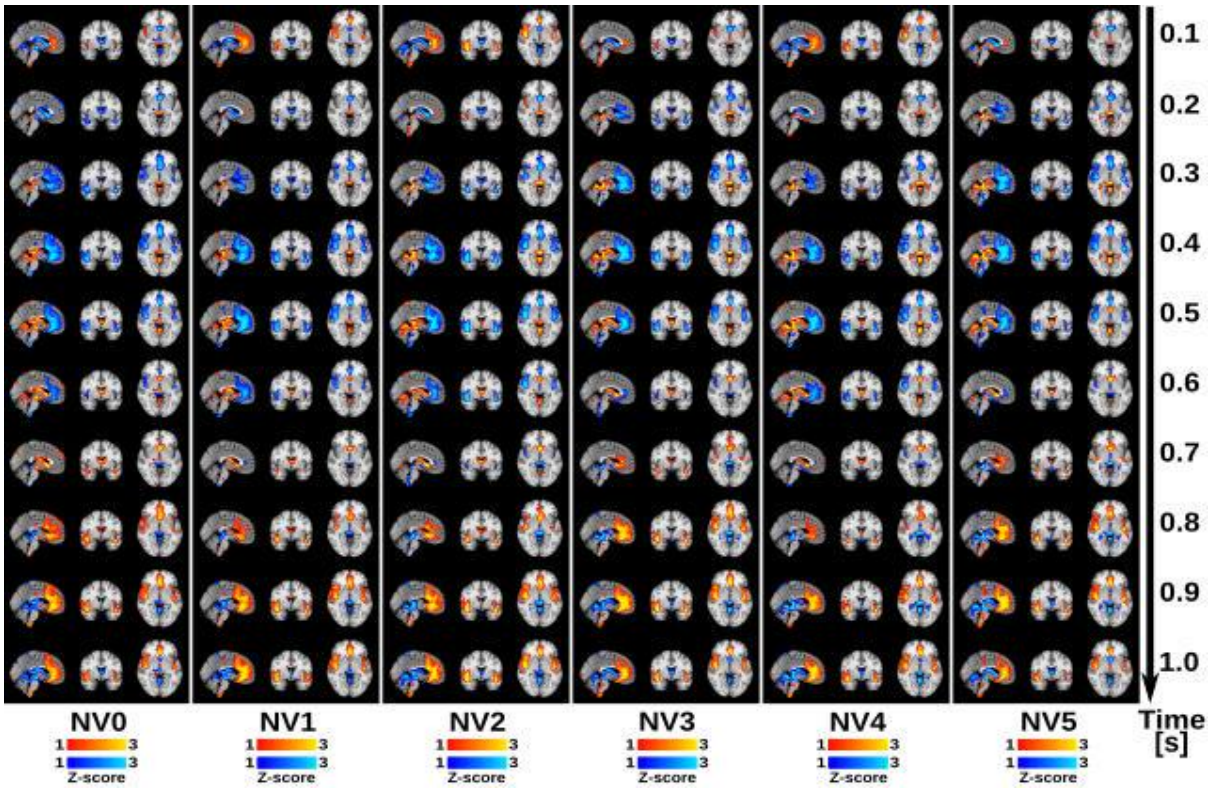

Supplementary_figure_6